Biometric Authentication System based on Hand Geometry and Palmprint Features

Laura Gulyás Oldal and András Kovács
John von Neumann Faculty of Informatics, Óbuda University, Budapest, Hungary

Keywords: Palmprint, Hand Geometry, Biometric Authentication.

Abstract: In today's society, biometric authentication has gained more significance, since it uses physical characteristics of a person for identification. Physical features provide greater security compared to ownership or knowledge based factors. More and more physiological measures prove to be great characteristics for personal authentication. A multimodal biometric authentication system has the advantage of using multiple physical characteristics for authentication achieving greater accuracy. If one modality fails to identify a person with high accuracy, other modalities are employed. However, in these kind of systems, every modality has a different imagery data requirement, which provides multiple captured images for evaluation. The method described in the article uses the same input data for processing multiple physiological features at once. Biometric characteristics used by the system are hand geometry and palmprint features. The imagery data requirement is a high-resolution image of a well-lit hand with dark background. Capturing the image in good sanitary conditions has become an important requirement in the past few years. Advantage of a high-resolution image compared to images captured with dedicated hardware devices like fingerprint or palmprint scanners, is contactless capturing of the image. Another benefit of a high-resolution camera usage is lower cost claims compared to the other systems using dedicated hardware for image capturing.

1 INTRODUCTION

Biometric authentication has become an important topic in security systems, as it is used for automated identification, criminal or forensic applications and access control systems. Some of the physiological features of a person suitable for authentication are fingerprint, palmprint, palm vein features, face characteristics, hand geometry features, etc. (Golfarelli, 1997).

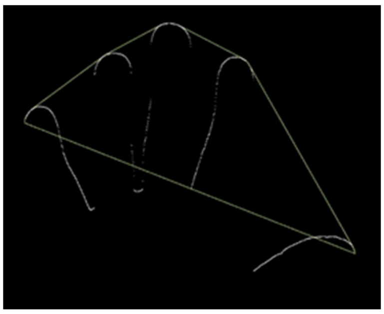

Figure 1: The convex hull of the point set after the auxiliary point removal.

A palmprint consists of multiple characteristics suitable for authentication, such as: wrinkles, epidermal ridges and principal lines. The principal lines of a palm provide quality measures for identification with high confidence. Some of the hand geometry features, appropriate for identification are finger lengths, and widths, maximal inscribed circle radius, palm area, width and height, finger proportions, etc. Features of the hand and palm can be extracted from a single high-resolution image. The aggregation of hand geometry and palmprint features in the system provides a more reliable authentication system using only one imagery data. The proposed method is an improved version of our previously published work (Gulyás Oldal, 2020). The main improvements of the current method are simpler keypoint detecting algorithms and testing the method on a much larger data set. The simplified algorithms provide the same results as the original solution, but with a much smaller margin of error. Another improvement made in the current version of the method is the performance improvement of key point detection. As the key point detecting algorithms do not require a high resolution image, the algorithms

Oldal, L. and Kovács, A.
Biometric Authentication System based on Hand Geometry and Palmprint Features.
DOI: 10.5220/0010408900580065
In *Proceedings of the International Conference on Image Processing and Vision Engineering (IMPROVE 2021)*, pages 58-65
ISBN: 978-989-758-511-1

use a downsized version of the original image, which results in much shorter run time.

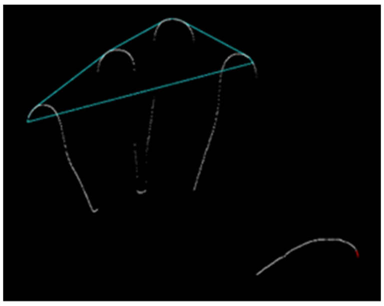

Figure 2: Two categories of the hull.

The imagery data requirement for the proposed method is a high-resolution image containing the entire hand, the foreground has to be well lit, while the background has to be as dark as possible. Another prerequisite of the image is the vertical orientation of the hand, as the image is not rotated during keypoint detection.

2 RELATED WORKS

In this section we give a brief overview of some methods using hand geometry or palmprint features for personal authentication.

In (Badrinath, 2012) the authors propose a method for palmprint based recognition where the palmprint is divided into several blocks, which are further processed using principal component analysis (PCA). The features used for matching are the phase-differences of the vertical and horizontal phase. The feature matching algorithm computes the Hamming distance of features and uses the given values for the calculation of matching score. The method has an EER (equal error rate) value of 0.25%.

Method described in (Li, 2012) uses a unique approach for palmprint matching. The authors of the paper consider the improper alignment of ROI-s of two palmprints to be the biggest flaw of most existing palmprint matching methods. The correct alignment of the ROI-s is achieved by extracting the palmprint principal lines and computing the adequate rotation and translation values with ICP (Iterative Closest Point) algorithm. Given the properly aligned palmprint images, an arbitrary method for palmprint feature extraction and recognition method is used. The authors achieved the best results using the CompCode (Huang, 2008) method, which uses Gabor filters in six different orientations for the direction estimation of palmprint image points. The CompCode method alone has an EER value of 0.0388%, while in joint with the proposed method had an EER value of 0.0201%. The additional step results in increased feature extraction and matching time as well.

The method proposed in (Badrinath, 2012) shows great results, however, the authors assume the proper alignment of the ROI-s. In (Li, 2012) method the authors propose a method for proper feature map alignment using the palmprint principal lines. The method is used as an additional step of existing palmprint recognition methods. The features extracted for ROI alignment and palmprint matching may differ. Our method uses a similar approach, however, the palmprint principal lines are used for ROI alignment and palmprint matching as well, which results in a simpler implementation of a palmprint recognition system.

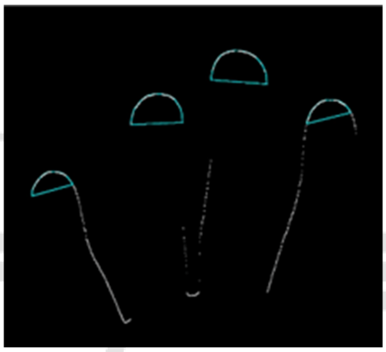

Figure 3: 4 subcategories of the second group and classified points.

3 HAND GEOMETRY CHARACTERISTIC POINT DETECTION

3.1 Preprocessing

The preprocessing of the imagery data consists of gray scaling, downsizing, binarization, noise removal and morphological edge detection. The key point detection does not require a high resolution image, therefore, the original image is downsized. This step provides greater efficiency for keypoint detecting algorithms and hand geometry feature extraction. The palm feature extracting algorithms are executed on the original image, as the palm lines require high resolution image for extracting quality principal line features. Subsequently, the downsized image is binarized with a threshold determined by Otsu's method. Having very different intensities of the foreground and background insures satisfactory results using Otsu's algorithm (Xu, 2011). As the binarized image contains significant amount of noise, the most effective method for noise removal is blob detection followed by filtering the largest blob (Grycuk, 2014). The extracted blob is the object defined by the shape of hand. This is an improvement of the previously published method, it is less sensitive to lighter areas of the background. The original method used median-filter for reducing noise, which proved to be effective only on inputs having almost completely black background. Any reflected light from the background causes non salt and pepper noise. The median-filter is not an effective method for the removal of bigger noise objects, consequently, this step had to be introduced.

Figure 4: The reduced point set for finger valley detection.

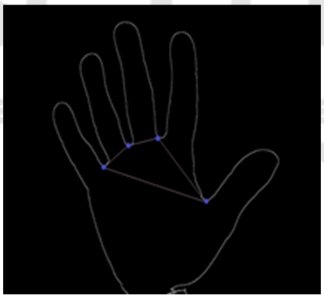

Figure 5: The output of the finger valley detection.

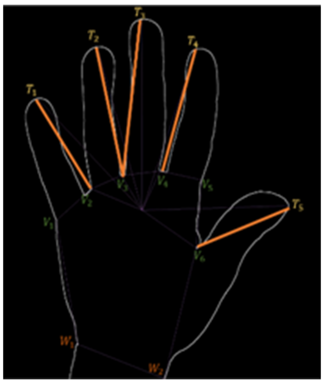

Figure 6: Calculated finger lengths.

Figure 7: Calculated maximal inscribed circle.

The next step of preprocessing the image is morphological edge detection. The morphological operations used for one-pixel thick edge extraction are erosion and subtraction (Hsiao, 2005) (Maksimović, 2020).

3.2 Fingertip Detection

Given the image containing one-pixel thick edges, the algorithm determines the fingertips. The set of edge points is reduced by retrieving the topmost points of every column on the image. The hull displayed on Fig. 1 is determined by multiple operations including Graham scan (Graham, 1972). With the analysis of the distances between successive points, the right or left orientation of the hand can be determined.

Subsequently, the hull points are classified to the following two groups:

- group of thumb points
- group of remaining four fingertip points.

The two categories are displayed on Fig. 2, the points of thumb are marked with red color, while the other category is marked with a blue color. The middle point from the first group is selected and represents the fingertip of the thumb. The second category is divided to four additional groups displayed on Fig. 3, and the remaining four fingertips are determined by selecting the local maxima from every group.

3.3 Wrist Point Detection

Wrist point detection is essential for hand area computation as the image section below the wrist cannot be included during hand area computation. The mentioned image section is not part of the hand, but the arm. The wrist point detection method described in (Gulyás Oldal, 2020) proved to be inaccurate in case of inadequate light conditions on the imagery data. The algorithm described below proved to be much more effective in different light conditions.

The detection starts with extraction of the leftmost and rightmost edge points in each row, followed by filtering the points below the thumb. The average distances between the rightmost and leftmost points are calculated for every row considering former n distances as well.

The wrist points are determined by the points with the biggest rate of change of average distances.

3.4 Finger Valley Detection

The finger valley search starts with elimination of leftmost and rightmost points from the set of edge points.

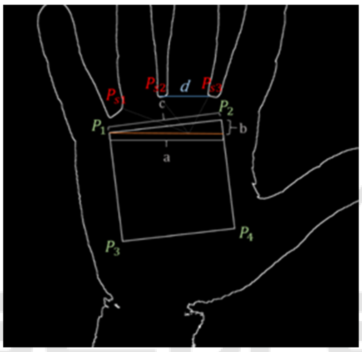

Figure 8: Points for ROI extraction.

The edge points are reduced further by defining a circle, as follows:

- Centre: COM
- Radius: $k \cdot dist(COM, middle\_finger\_tip)$,

where COM is the center of mass of the hand, $dist(COM, middle\_finger\_tip)$ the distance between the tip of middle finger and center of mass and k a free parameter ($k = 0.55$ in the implemented algorithm). The points inside the circle are kept, the remaining points are eliminated. The filtered point set is displayed on Fig. 4.

The following steps of finger valley detection include blob detection. The blobs extracted are four objects, where every blob contains points of one valley (Grycuk, 2014)[4]. The valleys between the fingers are finally determined by discovering the local minimum for every object. The detected finger valley points are displayed on Fig. 5. The process of valley detection is significantly simplified compared to the original version (Xu, 2014), as the initial method had a large margin of error. The original process of valley detection comprised of multiple steps built on each other, which made the algorithm more error prone. The improved method determines the points of valleys independently from each other.

4 HAND GEOMETRY FEATURES AND MATCHING

Absolute hand geometry measurements like finger proportions, lengths or maximal inscribed circle need to be calculated with respect to other measurements for the features to be resolution independent (Rutkowski, 2014).

The features considered during matching are the following:

- Finger length proportions (with respect to the middle finger length)
- Area of the largest inscribed circle (with respect to the area of the hand) (Sanchez-Reillo, 2000)
- Middle finger length (with respect to the area of the hand) (Bača, 2012)

The considered finger lengths are the distances between fingertip and finger valley points. Points used for finger length calculation are displayed on Fig. 6. The proportion of finger lengths characterize well a hands geometrical characteristics. Finger length proportions are a good descriptor of the hand's geometrical attributes (Sanchez-Reillo, 2000).

The finger length proportions are calculated with respect to the middle finger length, as it proved to have steadiest position among the fingers.

Another great descriptor of the hand shape is the area or radius of the largest inscribed circle (Sanchez-Reillo, 2000).

In the implemented solution, the largest inscribed circle is determined with a modified hill climbing algorithm (Kumar, 2003) (Ohashi, 2003). The detected circle with this method is displayed on Fig. 7. The similarity between two hands geometrical features is computed with the following formulas:

$$\boldsymbol{F} = t_{0.85,1}\left(\frac{1}{4}L'_1 + \frac{1}{4}L'_2 + \frac{1}{4}L'_3 + \frac{1}{4}L'_4\right) \cdot 100 \quad (1)$$

$$\boldsymbol{A} = t_{0.8,1}(T'_{MIC}) \cdot 100 \quad (2)$$

$$\boldsymbol{L} = t_{0.6,1}(L'_F) \cdot 100 \quad (3)$$

$$\boldsymbol{H} = \frac{\mathbf{2}}{\mathbf{8}}\boldsymbol{A} + \frac{\mathbf{3}}{\mathbf{8}}\boldsymbol{F} + \frac{\mathbf{3}}{\mathbf{8}}\boldsymbol{L} \quad (4)$$

Where:

- L'_i – i-th finger length proportion difference
- T'_{MIC} – maximal inscribed circle area difference
- L'_F - middle finger length difference

- $t_{a,b}(x) = \frac{x-a}{b-a} - a$function, which normalizes the input to the $[a, b]$ range
- F – finger proportion similarity
- A – maximal inscribed circle area difference
- L – finger length difference
- H – total hand geometry similarity

The weights of measurements considered during similarity level calculation are defined with respect to the steadiness of the feature.

5 PALMPRINT EXTRACTION AND MATCHING

5.1 Region of Interest (ROI) Extraction

The palmprint analysis starts with determining an image section, where the principal palm lines should be analyzed (Tóth, 2020). A square ROI is chosen in the proposed method, as two points (P_1, P_2) are sufficient for the determination of the whole square. The remaining two points calculated from P_1, P_2 points are P_3, P_4 marked on Fig. 8.

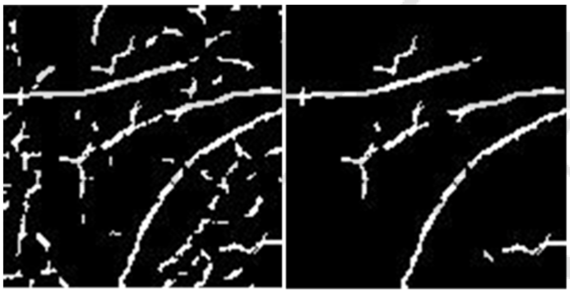

Figure 9: A binary image of extracted palm line before and after additional noise removal.

Figure 10: Dilated palm line images and the intersection.

$$\boldsymbol{P_1}\ (x_{P_{S1}} - \frac{d}{4}, x_{P_{S1}} + \frac{d}{2}) \tag{5}$$

$$\boldsymbol{P_2}\ (x_{P_{S3}} + \frac{d}{4}, x_{P_{S3}} + \frac{d}{2}) \tag{6}$$

$$\boldsymbol{P_3}(x_{P_1} + b, y_{P_1} + a) \tag{7}$$

$$\boldsymbol{P_4}(x_{P_2} + b, y_{P_2} + a) \tag{8}$$

On Fig. 8 the P_{S1}, P_{S2}, P_{S3} are the points of finger valleys, and d the vertical distance between the P_{S2} and P_{S3} valleys.

5.2 Palmline Extraction

The palmline extraction method is highly inspired by the (Bruno, 2014) study. After the extraction of the ROI image section on the original image, the palm image is downsized to 128·128 size, the method described below produces best results on small resolution image. The process is followed by gray scaling, contrast stretch and smoothing. Averaging filters are applied on the processed image with 4 different averaging filters with a mask size of 5·5. The different averaging filters smooth the palm lines in different directions, which are vertical, horizontal and two diagonal directions (Lin, 2016). On the resulting images a bottom hat filter is applied. The four resulting images are consolidated into one image by addition of the partial results (Bruno, 2014). The process is followed by the elimination of low intensity pixels, thresholding and noise removal for the purpose of erasing isolated spikes and blocks (Bruno, 2014). The method produces satisfying results, however, a considerable amount of noise was present on the output images (Fig. 9).

An alternative noise removal method had to be introduced, which is filtering the blobs in the palm image by height, width and area (Grycuk, 2014). The discontinuity of palm lines requests an additional step which is extending every blob larger than a certain size with a certain number of pixels. Following this step, the blobs are filtered by height, width and area. This method eliminates larger noise objects, which were not connected to the main palm lines during line extension. An essential last step is the removal of the added pixels on the filtered image.

5.3 Palmprint Matching

The result of palm line extracting algorithms were grayscale images containing the principal lines of the palm. Template matching is the initial step of palm image comparison. Points of the two images are linked based on the similarity of the surrounding pixels (Yuan, 2011).

The output of template matching is linked pairs of points containing true matches and mismatches (Hisham, 2015) (Kertész, 2018). The linked points are further filtered with RANSAC (Random Sample Consensus) algorithm. The algorithm creates a homography matrix based on the inlier pairs of points (Batyrshin, 2019) (Baráth, 2019).

With the use of homography matrix, an affine transformation is performed on one of the input images (Yaniv, 2010). With this method the feature points of one image are projected to the other input. However, the projected image and the reference image might not completely overlap, the two images are dilated and the intersection is computed from the two. (Fig. 10). The highest intensity image sections are the most relevant during matching, as these represent the main principal lines. The pixels which are taken into consideration are the pixels which satisfy the following condition:

$$Img(x,y) > k \cdot M_{!0} \tag{9}$$

where $M_{!0}$ is the mean intensity value of non-black pixels and k is a free parameter (k = 1.7 in the proposed method). The presence of the extracted pixels on the intersection determines the similarity level of the two palms.

6 COMBINING HAND GEOMETRY AND PALMPRINT

The result of the palmprint matching and hand geometry feature matching are summarized into one single value considering the quality of the extracted features (Dubrofsky, 2009). Therefore, different weights are used for the consolidation of the partial results.

$$\boldsymbol{S = 0.2\,H + 0.8\,P} \tag{10}$$

where:

- S – total similarity score
- H – similarity score of hand geometry features
- P – similarity score of palm features

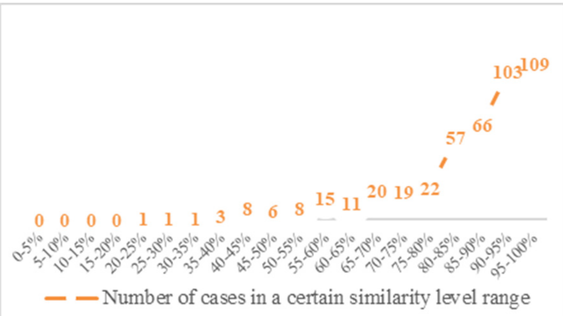

Figure 11: Similarity levels of cases given identical hands.

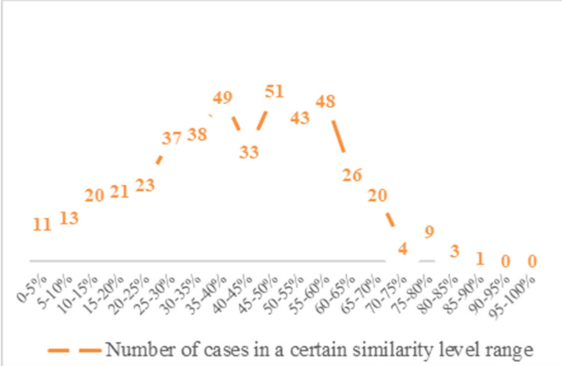

Figure 12: Similarity levels of cases given different hands.

7 RESULTS

The algorithms were tested on 214 2592·1944 resolution images of 14 different subjects.

The ages of the subjects vary from 20 to 60, half of the subjects are females, and the other half are males. The outcome of keypoint detection was tested and analyzed manually.

Subsequently, the feature extraction and feature matching was tested on 450 combinations given identical hands, and 450 combinations given different hands.

The results of the algorithm on identical subjects is shown on Fig. 11, while the results considering different subjects is shown on Fig. 12.

Considering the distribution of similarity levels given identical hands, it can be said, that in 75% of cases the algorithm confirmed an identity of a person with high confidence. The similarity level in these cases fell in the 80-100% range. In more than 96% of differing hand combinations, the method resulted with a similarity level between 0% to 70%, while in most cases the similarity level falls in the 30-60% range. The results suggest, that the algorithm in majority of different hand cases produces a value very different compared to identical hands.

This behavior allows us to view the effectiveness of the proposed method by analyzing FAR (False Acceptance Rate) and FRR (False Rejection Rate) on different acceptance thresholds (Ross, 2004). In Fig. 13. the FAR and FRR percentages are displayed considering a few acceptance thresholds. By defining 68% as the acceptance threshold, FAR (False Acceptance Rate) is 4.6%, and FRR (False Reject Rate) is 14,2%.

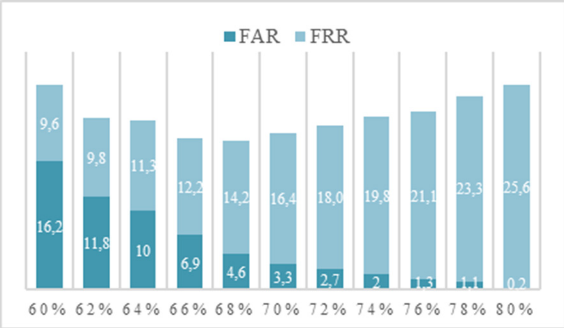

Figure 13: FAR and FRR considering different acceptance thresholds.

8 CONCLUSION

The method described in the paper provides a simple solution for a low-cost contact-free authentication system based on palmprint and hand geometry features. The implemented method produced promising outcome and enthuses further development. A future work for the method is an improvement of the palm feature matching algorithm, where the method will use distance transform for determining the similarity of the palm features following the affine transformation of one of the palm images. This improvement would provide a solution, where the varying intensities of palm lines would affect the effectiveness of the method to a lesser extent. A further future work for the method consist of improving the hand geometry feature matching. In the future, the method will use a machine learning algorithm for determining the optimal weights considered during matching with a machine learning algorithm. The current method in comparison with the previously published method (Gulyás Oldal, 2020) is significantly simpler, and therefore less error prone. The keypoint detection takes place on a downsized image, which made a significant difference in the run time of the algorithms. Furthermore, valley detection consists of independent simple steps, which proved to have a smaller margin of error and is much faster. During hand geometry feature matching, largest inscribed circle area is considered in replacement of the palm area, as the determination of the latter consisted of determining two additional root points of the fingers.

The two points could not be determined with high confidence, only a rough estimation was made. This resulted in a deviating palm area in different image samplings, and made the hand geometry feature matching less accurate. The method was tested on a significantly larger data set, which gives a better overview of the method's accuracy.

REFERENCES

Laura Gulyás Oldal, András Kovács, "Hand geometry and palmprint-based authentication using image processing," *2020 IEEE 18th International Symposium on Intelligent Systems and Informatics (SISY)*, Subotica, Serbia, 2020, pp. 125-130

Alessandro Bruno, Paolino Carminetti, Gentile Vito, Marco La Cascia, Emanuele Mancino, "Palmprint principal lines extraction" BIOMS 2014 - 2014 IEEE Workshop on Biometric Measurements and Systems for Security and Medical Applications, Proceedings, 2014

Xiangyang Xu, Shengzhou Xu, Lianghai Jin, Enmin Song, "Characteristic analysis of Otsu threshold and its applications" Pattern Recognition Letters, Vol. 32., 2011, pp. 957-960I.

Rafal Grycuk, Marcin Gabryel, Marcin Korytkowski, Rafal Scherer, and Sviatoslav Voloshynovskiy, "From Single Image to List of Objects Based on Edge and Blob Detection", *Lecture Notes in Computer Science*, 2014, pp. 605-615

Ying-Tung Hsiao, Cheng-Long Chuang, Joe-Air Jiang and Cheng-Chih Chien, "A contour based image segmentation algorithm using morphological edge detection," *2005 IEEE International Conference on Systems, Man and Cybernetics*, Waikoloa, HI, 2005, pp. 2962-2967 Vol. 3

Vladimir Maksimović , Branimir Jakšić , Mile Petrović , Petar Spalević, Mirko Milošević, "Analysis of Edge Detection on Compressed Images with Different Complexities", Acta Polytechnika Hungarica, Vol. 17, No. 4, 2020

Ronald L. Graham, "An Efficient Algorithm for Determining the Convex Hull of a Finite Planar Set", Information Processing Letters, Vol 1., 1972, pp. 132-133

Rutkowski, L., Scherer, R., Korytkowski, M., Pedrycz, W., Tadeusiewicz, R., Zurada, J.M. Artificial Intelligence and Soft Computing, ICAISC 2014, Lecture Notes in Computer Science 2014, vol 8468.

Raul Sanchez-Reillo, Carmen Sanchez-Avila, Ana-Gonzalez-Marcos, "Biometric Identification through Hand Geometry Measeurements", IEEE Transactions on Pattern Analysis and Machine Intelligence, Vol. 22, 2000, pp. 1168-1171Y.

Miroslav Bača, Petra Grd, Tomislav Fotak, New Trends and Developments in Biometricsm, Chapter 4: Basic Principles and Trends in Hand Geometry and Hand Shape Biometrics, 2012

Ajay Kumar, David C. M. Wong , Helen C. Shen, and Anil K. Jain, "Personal Verification Using Palmprint and Hand Geometry Biometric", Audio- and Video-Based Biometric Person Authentication, 2003, pp. 668-678

Takumi Ohashi, Zaher Aghbari, Akifumi Makinouchi, "Hill-Climbing Algorithm for Efficient Color-Based

Image Segmentation", Signal Processing, Pattern Recognition, and Applications, 2003

Bence Tóth Tamás, Sándor Szénási, "Tree Growth Simulation based on Ray-Traced Lights Modelling", Acta Polytechnika Hungarica, Vol. 17, No. 4, 2020

Lin, Sen & Xu, Tianyang & Yin, Xinyong. Region of interest extraction for palmprint and palm vein recognition. 9th International Congress on Image and Signal Processing, BioMedical Engineering and Informatics (CISP-BMEI), 2016, 538-542.

Weiqi Yuan,Sen Lin, Haibin Tong, Shudong Liu, "A Detection Method of Palmprint Principal Lines Based on Local Minimum Gray Value and Line Following" , *International Conference on Hand-Based Biometrics*, 2011

M. B. Hisham, Shahrul Nizam Yaakob, Raof R. A. A, A.B A. Nazren, N.M.Wafi, "Template Matching Using Sum of Squared Difference and Normalized Cross Correlation", *2015 IEEE Student Conference on Research and Development (SCOReD)*, 2015

Gabor Kertész, Sándor Szénási, Zoltán Vámossy, "Multi-Directional Image Projections with Fixed Resolution for Object Matching", Acta Polytechnika Hungarica, Vol. 15, No. 2, 2018

Ildar Z. Batyrshin ,"Constructing Correlation Coefficients from Similarity and Dissimilarity Functions", Acta Polytechnika Hungarica, Vol. 16, No. 10, 2019

Baráth Dániel, Matas Jiri, "Gráf-vágás RANSAC", KÉPAF 2019: Képfeldolgozók és Alakfelismerők Társaságának 12. országos konferenciája, 2019

Ziv Yaniv, Random Sample Consensus (RANSAC) Algorithm, A Generic Implementation, Imaging Science and Information Systems (ISIS) Center, Dept. of Radiology, Georgetown University Medical Center, Washington, DC, USA, 2010

Elan Dubrofsky, Homography Estimation, A Master's Essay Submitted in Partial Fulfillment of the Requirements for the Degree of Masters of Science in the Faculty of Graduate Studies, The University of British Columbia, 2009

A. Ross and A. K. Jain, "Multimodal biometrics: An overview," *2004 12th European Signal Processing Conference*, Vienna, 2004, pp. 1221-1224.

M. Golfarelli, D. Maio and D. Malton, "On the error-reject trade-off in biometric verification systems," in *IEEE Transactions on Pattern Analysis and Machine Intelligence*, 1997, vol. 19, no. 7, pp. 786-796

Huda, Syamsul; Yusuf, Enjang Burhanudin: Biometrics in the Quran Perspective: Definition, History, and Type. *Didaktika Religia*, December 2019, pp. 276-298

G.S. Badrinath, Phalguni Gupta: Palmprint based recognition system using phase-difference information, *Future generation Computer Systems*, Vol. 28 No. 1, January 2012, pp. 287-305

Wei Li, Bob Zhang, Lei Zhang and Jingqi Yan: Principal Line-Based Alignment Refinement for Palmprint Recognition, *IEEE Transactions on Systems, Man, and Cybernetics, Part C (Applications and Reviews)*, Vol. 42, No. 6, November 2012, pp. 1491-1499

De-Shuang Huang, Wei Jia, David Zhang: Palmprint verification based on principal line, *Pattern recognition*, Vol 41. No. 4, April 2008, pp. 1316-132